Sorting Single-Walled Carbon Nanotubes by Electronic Type Using Nonionic, Biocompatible Block Copolymers

Alexander L. Antaris, Jung-Woo T. Seo, Alexander A. Green, and Mark C. Hersam*

Department of Materials Science and Engineering and Department of Chemistry, Northwestern University, Evanston, Illinois 60208-3108

ABSTRACT As-synthesized single-walled carbon nanotubes (SWNTs) typically possess a range of diameters and electronic properties. This polydispersity has hindered the development of many SWNT-based technologies and encouraged the development of postsynthetic methods for sorting SWNTs by their physical and electronic structure. Herein, we demonstrate that nonionic, biocompatible block copolymers can be used to isolate semiconducting and metallic SWNTs using density gradient ultracentrifugation. Separations conducted with different Pluronic block copolymers reveal that Pluronics with shorter hydrophobic chain lengths lead to higher purity semiconducting SWNTs, resulting in semiconducting purity levels in excess of 99% obtained for Pluronic F68. In contrast, X-shaped Tetronic block copolymers display an affinity for metallic SWNTs, yielding metallic purity levels of 74% for Tetronic 1107. These results suggest that high fidelity and high yield density gradient separations can be achieved using nonionic block copolymers with rationally designed homopolymer segments, thus generating biocompatible monodisperse SWNTs for a range of applications.

KEYWORDS: carbon nanotube · separation · sorting · biotechnology · Pluronic · Tetronic · density gradient ultracentrifugation

The production of carbon nanotubes with controlled atomic and electronic structure has led to devices with improved performance[1−5] and functionality,[6] and enabled a more detailed understanding of the physical properties of these one-dimensional nanomaterials.[7−10] While significant advances have been achieved in recent years,[11] it remains a considerable challenge to generate carbon nanotubes with controlled structure. Synthetic methods can achieve some degree of control over the distribution of nanotube chiralities[12] and electronic type;[13] however, further improvements in growth are required for optimal performance in devices. To address this issue, a number of postsynthetic methods for sorting carbon nanotubes according to their diameter, wrapping angle, and electronic type (metallic *versus* semiconducting) have been developed.[14−18] For instance, a large number of polymers and biomolecules, such as PFO,[19] single-stranded DNA,[20,21] and flavin mononucleotide,[22] adopt SWNT-structure-dependent configurations around single-walled carbon nanotubes (SWNTs), which can be exploited to enable isolation according to SWNT structure. The SWNT structural specificity of these molecules is generally attributed to their ability to self-associate and form sheath-like structures that conform with the atomic structure of a given SWNT species.

One of the most widely used methods for separating SWNTs is density gradient ultracentrifugation (DGU).[23] This technique exploits differences in the buoyant density of surfactant-encapsulated SWNTs, which translate into differences in the position of the SWNTs within a density gradient once they are subjected to high centripetal forces. Previous work[1,6] has shown that by varying the levels of the anionic surfactants sodium cholate and sodium dodecyl sulfate, it is possible to isolate SWNTs according to their diameter and/or their electronic type with purity levels for the latter exceeding 99%. Despite some experimental[17,24−26] and theoretical[27] studies, the surfactant-SWNT interactions that enable DGU separations, particularly those by electronic type, are not well understood. This limited understanding is due in part to the difficulty in faithfully simulating a typical DGU experiment, which involves the complex interplay between SWNTs, different mixtures of competing surfactant species, counterions, water molecules, and density gradient media. In the absence of a predictive theoretical model, efforts to improve the fidelity and yield of DGU separations will benefit from detailed experimental protocols and data that explore the vast phase space for this technique.

*Address correspondence to m-hersam@northwestern.edu.

Received for review June 17, 2010 and accepted July 23, 2010.

Published online July 29, 2010.
10.1021/nn101363m

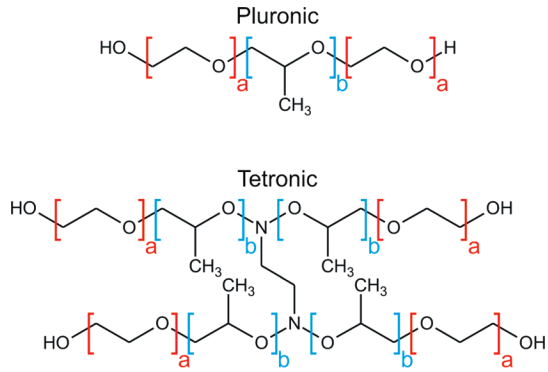

Figure 1. Chemical structures of Pluronic and Tetronic block copolymers.

Herein, we present a comprehensive series of DGU electronic type separations utilizing two distinct classes of nonionic, biocompatible block copolymers: Pluronics and Tetronics. Pluronics are linear copolymers composed of a central hydrophobic polypropylene oxide (PPO) group flanked by two hydrophilic polyethylene oxide (PEO) chains (Figure 1). Tetronics, on the other hand, are X-shaped copolymers formed by four PPO−PEO blocks bonded to a central ethylene diamine linker (Figure 1). Unlike the anionic surfactants typically employed in DGU separations, both block copolymer classes are available in a large number of different structural permutations established through independent and systematic control of their hydrophilic and hydrophobic chain lengths. Pluronic−SWNT suspensions have generated recent interest because of their biocompatibility,[28−31] self-assembly,[32,33] and amenability to theoretical modeling.[34−36] Previous studies have shown that the dispersion efficiency of a Pluronic depends strongly on the length of the PEO and PPO copolymer segments[37] and that the hydrophobic PPO chains adhere to the SWNT surface while the hydrophilic chains extend into solution.[32,35,37]

Beyond providing an alternative, biocompatible chemistry for DGU, our results shed light on the interactions between block copolymers and SWNTs. The buoyant density of the copolymer−SWNT complex varies as a function of the diameter, wrapping angle, electronic type, and bundling of the SWNTs, the ordering and surface coverage of the copolymer on the SWNT sidewalls, and the organization of water and hydrophilic polymer regions in the outer region of the complex. Following DGU, the buoyant density of the separated SWNTs is measured directly, and the SWNT chirality distribution is determined spectroscopically. Hence, DGU provides an exquisitely sensitive platform upon which to characterize copolymer−SWNT interactions, particularly as a function of SWNT diameter and electronic type. In this paper, Pluronics and Tetronics are found to possess a differential affinity as a function of SWNT electronic type (*i.e.*, semiconducting *versus* metallic). Furthermore, the yield and purity of the SWNTs following DGU varies systematically with the block copolymer structure, reaching purities greater than 99% for semiconducting SWNTs with Pluronic F68. These results show that nonionic block copolymers are a promising class of dispersion agents for DGU-based SWNT separations. In addition, the known biocompatibility of these nonionic block copolymers suggests new opportunities for monodisperse SWNTs in biotechnology applications such as biosensing, bioimaging, and drug delivery.

RESULTS AND DISCUSSION

DGU-based separations of arc discharge grown SWNTs were performed with Pluronic block copolymers at a concentration of 1% w/v in density gradients generated using iodixanol (see Materials and Methods). A homogeneous loading of Pluronic throughout the density gradient was essential for successful DGU separations, with the absence of Pluronic in the gradient inducing flocculation of most of the SWNTs during ultracentrifugation. This behavior is consistent with the Pluronic affiliated with the SWNTs being dynamically replaced by free Pluronic in solution. This dynamic interaction between Pluronic and SWNTs is qualitatively different from the wrapping configurations favored by other chain-like macromolecules such as single-stranded DNA, which are difficult to detach from the SWNT sidewalls.[38]

Following Pluronic-SWNT DGU separations, multiple bands are observed in the centrifuge tubes although their position, composition, and intensity varied considerably depending on the Pluronic used. Figure 2 panels a and c present photographs of the centrifuge tubes after DGU separations using Pluronic F108 and Pluronic F68, two copolymers that differ in both their PEO and PPO chain lengths. Immediately obvious are the differences in banding in both centrifuge tubes. Whereas the separation with Pluronic F108 results in a broad brown banding region with some variations in intensity down the tube, the separation with Pluronic F68 yields two distinct reddish bands separated by over 1 cm. The separated Pluronic-SWNT bands are fractionated layer by layer and characterized using optical absorbance spectroscopy.

Using these optical absorbance measurements, the composition of the Pluronic-SWNTs are mapped as a function of their position in the centrifuge tube, and hence their buoyant density. The arc discharge synthesized SWNTs used in these experiments have diameters ranging from 1.2−1.7 nm with an average diameter of ~1.5 nm. This diameter range produces optical absorbance peaks corresponding to semiconducting second order transitions between 900−1270 nm and first order metallic transitions between 600−850 nm. As a result, the electronic type purity of the SWNTs can be determined by comparing the areas under the metallic and semiconducting absorbance peaks with respect to a reference SWNT sample with a known composition.[6] In addition, variations in the diameter distribution of the

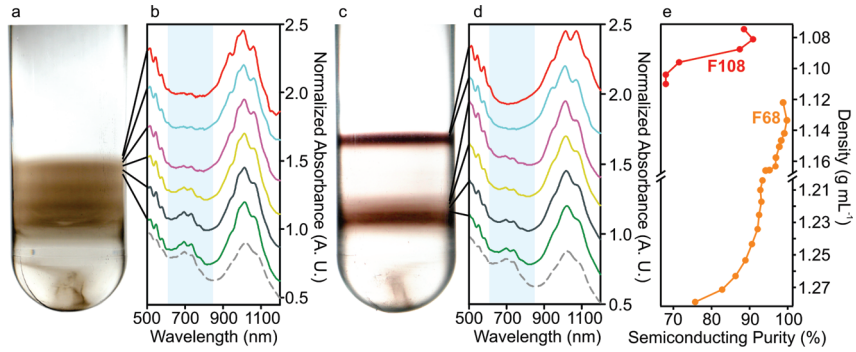

Figure 2. Separation of SWNTs using Pluronics. Photographs of centrifuge tubes following DGU separations with Pluronic F108 (a) and Pluronic F68 (c). Optical absorbance spectra of SWNTs extracted in the centrifuge tube at the locations labeled by black lines for Pluronic F108 (b) and Pluronic F68 (d) separations. Dashed gray curves are the absorbance spectra of unsorted SWNTs. The absorbance of metallic SWNTs in the blue shaded region changes as a function of the location in the centrifuge tube and indicates enrichment of semiconducting SWNTs. (e) Semiconducting SWNT purity level as a function of SWNT buoyant density for Pluronic F108 and Pluronic F68 separations.

SWNTs can be determined by changes in the wavelengths of the SWNT transitions as the energies of these excitations are inversely related to the SWNT diameter.

The optical absorbance spectra obtained from the Pluronic F108 and F68 DGU separations are shown in Figures 2b,d. Both copolymers yield enriched semiconducting SWNTs in the more buoyant fractions as evidenced by strongly suppressed first order metallic transitions. In particular, the Pluronic F68 DGU separation produces fractions with semiconducting purities exceeding 99%, compared to ~90% for Pluronic F108. Once the peak purity level is reached, the semiconducting purity decreases monotonically with increasing buoyant density until the SWNT composition is essentially identical to that of the unsorted SWNTs at 67% purity (Figure 2e). The Pluronic F68 separation also exhibits some diameter enrichment in the most buoyant fractions; however, this effect is relatively weak, especially in comparison to DGU-based SWNT separations employing anionic surfactants[1,6,39] or DNA.[40]

To better understand the source of differences in Pluronic separations, a series of DGU experiments were performed on 13 additional Pluronic copolymers, 7 of which stably encapsulated SWNTs under the ultracentrifugation conditions. Of the seven DGU-compatible Pluronics, all contain individual hydrophilic PEO chains longer than approximately 50 monomer units. This observation suggests that Pluronics with shorter hydrophilic chain lengths produce copolymer-SWNT complexes consisting of bundled SWNTs that are too dense for DGU processing or that shorter hydrophilic chains provide insufficient steric hindrance to prevent the SWNTs from rebundling during DGU.

Table 1 summarizes the principal findings of this survey of Pluronic-based DGU separations. First, the maximum purity of the semiconducting SWNTs separated using Pluronics is inversely related to the hydrophobic PPO chain length. Pluronic F127 (average PPO chain length of 65 monomers) extracted a maximum semiconducting purity of 82% while Pluronic F68 (average PPO chain of 29 monomers) yielded purities greater than 99%. Those Pluronics with intermediate PPO lengths also generally follow this trend (Figure 3). Second, decreasing the average number of hydrophobic PPO monomers resulted in greater semiconducting SWNT extraction efficiencies. For these experiments, the extraction efficiency is defined as the percentage of the total semiconducting SWNTs originally inserted into the density gradient that were extracted at a given semiconducting purity level after ultracentrifugation. Consequently, smaller PPO chain lengths not only produce higher purity material but are also more efficient

TABLE 1. Pluronic Semiconducting SWNT Sorting Efficiency

							semiconducting SWNT extraction efficiency				
Pluronic	PEO[a]	PPO[b]	MW[c]	isolated semi. band	buoyant density[d] (g/mL)	maximum purity (%)	>80%	>85%	>90%	>95%	≥99%
F127	100	65	12600	N	1.11	82	0.8	0	0	0	0
F108	133	50	14600	N	1.11	90	6.6	4.9	1.4	0	0
F98	118	45	13000	N	1.11	91	7.2	4.1	1.8	0	0
F88	104	39	11400	N	1.12	92	10.6	5.3	1.8	0	0
F87	61	40	7700	N	1.13	97	5.8	3.4	2.0	0.5	0
F77	53	34	6600	Y	1.14−1.16	97	24.9	13.6	7.9	1.6	0
F68	76	29	8400	Y	1.14−1.15	>99	35.3	26.1	17.8	11.3	3.9

[a]Average number of PEO monomers per chain. [b]Average number of PPO monomers per chain. [c]Mean molecular weight of the copolymer in Da as specified by BASF Corp. [d]Individual buoyant density values correspond to the end of the high purity semiconducting SWNT region while buoyant density ranges correspond to the high purity band of bimodal SWNT density distributions.

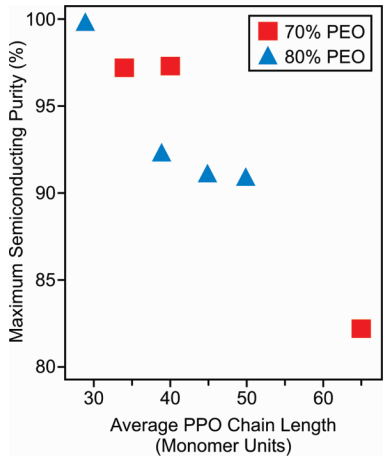

Figure 3. The maximum semiconducting SWNT purity level increases as the length of the hydrophobic PPO segment decreases. Pluronics with names ending in 7 and 8 consist of 70% and 80% PEO by molecular weight, respectively.

at capturing the sorted semiconducting SWNTs from the starting SWNT mixture. Deviations from the above trends are observed for a few of the Pluronics and likely can be attributed to differences in the ratio of hydrophilic to hydrophobic chain lengths.

This investigation of the Pluronic family also reveals that the general buoyant density-structure relationship in the Pluronic-SWNTs can be one of two types as suggested in Figure 2a,c. Pluronic F68 and Pluronic F77, the only DGU-compatible Pluronics with PPO chain lengths shorter than approximately 35 monomers, produced a relatively clear density gradient straddled by an isolated high purity semiconducting SWNT band at low buoyant density and a more heterogeneous SWNT band at high buoyant density. In contrast, DGU separations with the other Pluronics featured a high purity semiconducting SWNT region resting directly above the lower purity fractions. Interestingly, we found that lowering the concentration of Pluronic F108 during ultrasonication and the subsequent DGU separation also yields a bimodal density-structure relationship. Pluronic F108 separations at 0.3% w/v copolymer loading resulted in a maximum semiconducting purity of 94% in the isolated band, which corresponds to a 4% increase in purity compared to the 1% w/v loading separation. The increase in purity at low Pluronic concentration, however, is offset by a large decrease in extraction efficiency.

The observations above suggest that Pluronics can adopt two different configurations on the surface of the SWNTs. The single-mode buoyant density−structure relationships observed in the long PPO-chain Pluronics are likely caused by a disordered arrangement of copolymer at or near the SWNT surface. In this case, the individually encapsulated SWNTs have a similar copolymer arrangement as bundled SWNTs, which cause them to have comparable buoyant densities. This effect can be seen in the optical absorbance spectra of Figure 2b. The more buoyant individually encapsulated SWNTs exhibit sharper peaks compared to the denser, bundled SWNTs whose peaks are broader and red-shifted—both spectroscopic signs of increased bundling.[41] In contrast, Pluronic-SWNT systems that exhibit bimodal density-structure relationships likely have a subset of low buoyant density SWNTs that are coated by ordered copolymer layers. Such ordered Pluronic arrangements are suggested by the high electronic type sensitivity shown by Pluronic F68, which is unlikely to be obtained without strong copolymer-SWNT interactions, and their tight buoyant density distribution compared to lower purity SWNTs. Furthermore, the variations in the buoyant density distribution as a function of Pluronic F108 concentration demonstrate that the bimodal SWNT density distribution is sensitive to the levels of free copolymer in solution. This behavior can plausibly be attributed to a large excess of copolymer at higher loadings that increases the likelihood of random initial copolymer adsorption at multiple points on the SWNTs, thus frustrating ordered copolymer assembly.

Motivated by the high extraction efficiencies and purities afforded by Pluronic copolymers, a series of DGU separations were performed using Tetronic-encapsulated SWNTs. Tetronics were selected for study as each half of the X-shaped copolymer structurally resembles Pluronic with tertiary amine bridging elements as the only notable difference. In these copolymers, the hydrophobic PPO groups occupy the center of the surfactant while the hydrophilic PEO chains extend outward. Despite previous studies of star polymers[42,43] and the wide use of Pluronics,[30,32−35] Tetronic-SWNT dispersions have to our knowledge not been reported previously. Accordingly, SWNT extraction efficiencies were first determined for a series of Tetronics with varying PEO and PPO chain lengths. In agreement with previous Pluronic studies,[37] the SWNT dispersion efficiency of Tetronics depends strongly on PEO length (Figure 4a). Tetronic 1301 and Tetronic 901 disperse no SWNTs because of their high hydrophobicity and short PEO chain lengths (~4 monomers long). Tetronics with individual PEO chains longer than an average of 15 monomers show SWNT dispersion efficiencies near or above the level of the widely used anionic surfactant sodium dodecyl sulfate.

DGU separations with the most efficient Tetronics resulted in a noticeable green tint at the top of the SWNT banding region. Optical characterization of the separated SWNT fractions revealed that these SWNTs consist of up to 74% metallic species (Figure 4b)—a sizable increase in metallic SWNT content given the roughly one-third metallic distribution of the starting SWNT material. While a variety of structurally different Pluronics are compatible with DGU, the limited number of Tetronics that do not rebundle during DGU makes unraveling the relationship between structure and sorting ability difficult (Table 2). The maximum purity ap-

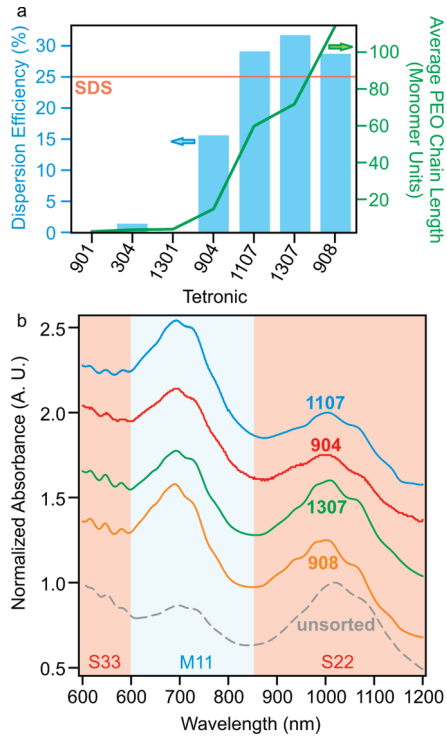

Figure 4. Dispersion and separation of SWNTs using Tetronics. (a) Plot of the SWNT dispersion efficiency of Tetronics as a function of average PEO chain length. For PEO segments greater than ~80 monomers in length, the dispersion efficiency of Tetronics exceeds that of the widely used nanotube surfactant sodium dodecyl sulfate (SDS), which has a dispersion efficiency of 25% under identical processing conditions. (b) Optical absorbance of the highest purity metallic fractions of Tetronic-sorted SWNTs. Normalization to the second-order semiconducting excitations (S22, shaded red) makes increases in the strength of the metallic transitions (M11, shaded blue) readily apparent in comparison to the unsorted SWNT absorbance (dashed gray). Third-order semiconducting transitions (S33) are also shaded red.

pears weakly dependent on the Tetronic copolymer size, since both of the Tetronics with the smallest molecular weight achieved greater than 65% pure metallic SWNT fractions while the second smallest Tetronic yielded metallic purities of up to 74%. Sorting efficiency at low purity (50%) directly relates to the PEO chain length. Unlike Pluronics, no isolated metallic bands were observed in the Tetronic density gradients after ultracentrifugation. All metallic SWNT-enriched regions were located directly above fractions that contain unsorted material and SWNT bundles.

Additional Pluronic and Tetronic separations were performed using smaller diameter CoMoCAT (~0.8 nm average diameter) and HiPco (~1.0 nm average diameter) SWNTs. Of these, only a HiPco separation in Pluronic F68 showed any degree of enrichment with a modest increase in semiconducting SWNT purity levels. Insight into the origin of this diameter dependence in the copolymer-SWNT interactions can be gained from theoretical calculations. In particular, recent coarse-grain Monte Carlo simulations of hard sphere chains confined to a cylindrical surface predict wrapping conformations that strongly depend on cylinder radii.[44–46] These results indicate that PPO chains may not adsorb strongly to small diameter SWNTs due to the high energetic and entropic costs for wrapping their sharply curved surfaces.

Finally, atomic force microscopy (AFM) was used to investigate the length distributions of the copolymer-sorted SWNTs (Figure 5). Greater than 99% purity semiconducting Pluronic-SWNTs had an average length of 920 nm while 74% metallic purity Tetronic-SWNTs were on average 680 nm long. Both classes of sorted SWNTs are sufficiently long for incorporation into SWNT network electronic devices with reasonable performance.[2,6] Regarding the observed ~25% difference in length between semiconducting Pluronic-SWNTs and metallic Tetronic-SWNTs, it should be noted that similar length differences are observed following electronic type DGU separations using anionic surfactants.[1] The greater polarizability of metallic SWNTs increases the van der Waals forces experienced by metallic SWNTs in bundled form and thereby leads to relatively shorter metallic SWNTs being freed from bundles during the ultrasonication that precedes DGU separations.

Overall, electronic type sorting of SWNTs with nonionic block copolymers can be attributed to two main factors. Similar to the behavior of ionic surfactants typically employed in DGU separations, the block copolymer hydrophobic core appears to have a preferential affinity to a particular SWNT electronic type.[17] For example, PPO selectively binds to semiconducting

TABLE 2. Tetronic Metallic SWNT Sorting Efficiency

						metallic SWNT extraction efficiency				
Tetronic	PEO[a]	PPO[b]	MW[c]	buoyant density[d] (mg/mL)	maximum purity (%)	>50%	>55%	>60%	>65%	>70%
908	114	21	25000	1.10	63	20.0	12.0	5.9	0	0
1307	72	23	18000	1.11	64	19.6	9.7	3.2	0	0
904	15	17	6700	1.13	67	4.9	3.0	1.9	1.2	0
1107	60	20	15000	1.11	74	13.4	8.8	6.0	4.1	2.5
304	3.7	4.3	1650							
901	2.7	18.2	4700							
1301	4	26	6800							

[a]Average number of PEO monomers per chain. [b]Average number of PPO monomers per chain. [c]Mean molecular weight of the copolymer in Da as specified by BASF Corp. [d]Individual buoyant density values correspond to the end of the high purity metallic SWNT region.

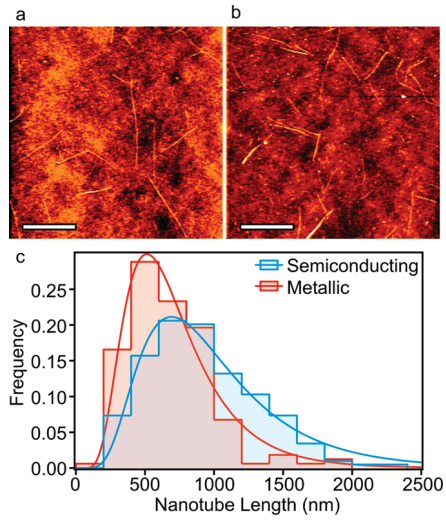

Figure 5. AFM images and length distribution data for DGU-sorted Pluronic and Tetronic encapsulated SWNTs. Representative 4 μm × 4 μm AFM images of semiconducting Pluronic-SWNTs (a) and metallic Tetronic-SWNTs (b) on SiO_2. Histograms displaying the length distribution of 204 and 164 individual SWNTs wrapped with Pluronic (c) and Tetronic (d), respectively. The Pluronic-sorted SWNTs have an average length of 916 nm, and the Tetronic-sorted SWNTs have an average length of 678 nm. Both length distributions are well represented by log-normal distribution functions, shown as solid curves. Scale bars in images a and b are 1 μm.

SWNTs as evidenced by the depletion of metallic SWNTs with Pluronic F68 in the most buoyant fractions (Figure 2d). Similarly, the affinity of Tetronic to metallic SWNTs may be attributed to its distinct hydrophobic core structure and the presence of dual tertiary amines found at the center of the hydrophobic segment. Unlike the smaller ionic surfactants, copolymer-based SWNT electronic type sorting also depends on the ability of the copolymer to form an ordered sheath around the SWNTs. While a more ordered copolymer-SWNT wrapping structure increases maximum extractible semiconducting purity when moving from 65 (F127) to 40 (F87) PPO monomer units, a wrapping structural transition between F87−F77 produces the bimodal distribution patterns observed in both F77 and F68. On the other hand, the lower maximum metallic purities achieved with Tetronic may be attributed to the inability of the X-shaped Tetronic to form a tightly packed and highly ordered conformation surrounding metallic SWNTs. While polymeric electronic type affinity and wrapping structure both influence electronic type sorting, other experimental results such as the apparent inability of commercially available Pluronics and Tetronics to sort small diameter HiPco or CoMoCAT SWNTs suggest that other parameters, such as SWNT diameter, can play a role. Fortunately, by exploiting the high degree of block copolymer tunability, further in-depth experimental studies in corroboration with theoretical modeling are likely to yield further insight into copolymer-based SWNT sorting mechanisms.

CONCLUSION

Nonionic, biocompatible block copolymers have been employed to sort SWNTs by electronic type using DGU. Greater than 99% purity semiconducting SWNTs are isolated using the linear block copolymer Pluronic F68, while 74% purity metallic SWNTs are isolated using the X-shaped block copolymer Tetronic 1107. Systematic studies of multiple Pluronics reveal that the SWNT semiconducting purity is correlated with the Pluronic hydrophobic and hydrophilic chain lengths, with increasing purity levels obtained for shorter hydrophobic blocks. Furthermore, the successful dispersion and separation of SWNTs using a range of Tetronics illustrate that these copolymers form a promising class of relatively unexplored nanotube dispersants.

Block copolymers provide a DGU system that is amenable to theoretical modeling and should assist in the development of more efficient carbon nanotube separation methods through simulation-driven surfactant design. Moreover, these experiments demonstrate how DGU can be utilized to investigate polymer-nanotube interactions as a function of polymer structure and nanotube diameter, electronic type, and wrapping angle. The high purity levels and biocompatibility of the SWNTs produced using nonionic block copolymers hold promise for a variety of applications ranging from electronics[2,3] to *in vivo* diagnostics or therapeutics.[30,47]

METHODS

Dispersion of SWNTs by Ultrasonication. P2 SWNTs synthesized by arc discharge (Carbon Solutions, Inc., batch number 02-376) were added to a 1% w/v block copolymer aqueous solution with a loading of ~1 mg mL^{-1}. The solution was subsequently horn ultrasonicated (Fisher Scientific model 500 Sonic Dismembrator) for 1 h at 20% of the maximum tip amplitude (~10 W). HiPco (Unidym, Inc.) and CoMoCAT (Southwest Nanotechnologies, Inc.) SWNT solutions were prepared in the identical manner.

Tetronic SWNT Dispersion Efficiency. Tetronic P2 SWNT solutions were dispersed in the above manner and ultracentrifuged in an SW41 Ti rotor (Beckman Coulter, Inc.) for 1 h at 41000 rpm and a temperature of 22 °C. Following ultracentrifugation, the top 7 mL of supernatant was carefully decanted and characterized using optical absorbance spectroscopy. Tetronic dispersion efficiencies were calculated by comparing the absorption strength of the decanted SWNT dispersion to that of the ultrasonicated SWNTs prior to ultracentrifugation. In particular, dispersion efficiencies were extracted at a wavelength of 1019 nm, which corresponds to the peak absorbance intensity of the P2 SWNT second-order semiconducting optical transitions.

Electronic Type Sorting *via* DGU. SWNTs were sorted by electronic type in density gradients containing a homogeneous 1% w/v copolymer loading. Density gradients consisted of the following layers beginning from the bottom of the centrifuge tube: a 4.5 mL, 60% w/v iodixanol under layer; a 15 mL linear density gradient ranging from 25−45% w/v iodixanol for all block copolymers other than F127, F108, and F98 (which were run in 20−40% w/v iodixanol gradients); 4 mL of 3% w/v iodixanol containing the dispersed SWNTs; and finally a 0% w/v iodixanol overlayer.

Before being added to the gradient, ultrasonicated SWNT solutions were centrifuged for 5 min at 15000 rpm (Eppendorf Centrifuge 5424) to remove macroscopic SWNT bundles. All centrifuge tubes for block copolymer sorting comparisons were run using a SW 32 Ti rotor (Beckman Coulter, Inc.) for 18 h at 32000 rpm and a temperature of 22 °C. Investigations of copolymer loading and SWNT diameter effects were run using scaled down density gradients in an SW 41 Ti rotor. Such separations were carried out for 12 h at 41000 rpm and 22 °C.

Fractionation and Optical Characterization. Fractions were collected in 0.5 mm steps using a piston gradient fractionator (Biocomp Instruments, Inc.). Optical cuvettes, diluted to a total volume of 0.850 mL using a 1% w/v block copolymer solution, were characterized by a Varian Cary 5000 spectrophotometer within 24 h of dilution.

Preparation of AFM Samples. Copolymer-wrapped SWNTs were deposited onto SiO_2-capped silicon wafers functionalized with (3-aminopropyl)triethoxysilane (Sigma-Aldrich) as described in ref 5.

AFM Imaging and Length Analysis. AFM images were acquired with a Thermo Microscopes Autoprobe CP-Research AFM operating in tapping mode. Conical AFM probes with a chromium−gold backside coating were used for all measurements (MikroMasch, NSC36/Cr−Au BS). Images of 4 μm × 4 μm size were taken to compute the length distributions of Pluronic- and Tetronic-encapsulated SWNTs. Overlapping and highly bundled nanotubes were excluded from the analysis.

Acknowledgment. This work was supported by the Army Research Office (W911NF-09-1-0233), the National Science Foundation (DMR-0520513, EEC-0647560, and DMR-0706067), and the Nanoelectronics Research Initiative. DGU instrumentation was funded by the Office of Naval Research (N00014-09-1-0180 and N00014-09-1-0795). A Natural Sciences and Engineering Research Council of Canada Postgraduate Scholarship (A.A.G.) is also acknowledged.

REFERENCES AND NOTES

1. Arnold, M. S.; Green, A. A.; Hulvat, J. F.; Stupp, S. I.; Hersam, M. C. Sorting Carbon Nanotubes by Electronic Structure Using Density Differentiation. *Nat. Nanotechnol.* **2006**, *1*, 60–65.
2. Engel, M.; Small, J. P.; Steiner, M.; Freitag, M.; Green, A. A.; Hersam, M. C.; Avouris, P. Thin Film Nanotube Transistors Based on Self-Assembled, Aligned, Semiconducting Carbon Nanotube Arrays. *ACS Nano* **2008**, *2*, 2445–2452.
3. Nougaret, L.; Happy, H.; Dambrine, G.; Derycke, V.; Bourgoin, J. P.; Green, A. A.; Hersam, M. C. 80 GHz Field-Effect Transistors Produced Using High Purity Semiconducting Single-Walled Carbon Nanotubes. *Appl. Phys. Lett.* **2009**, *94*, 243505.
4. Miyata, Y.; Yanagi, K.; Maniwa, Y.; Kataura, H. Highly Stabilized Conductivity of Metallic Single-Wall Carbon Nanotube Thin Films. *J. Phys. Chem. C* **2008**, *112*, 3591–3596.
5. Green, A. A.; Hersam, M. C. Processing and Properties of Highly Enriched Double-Wall Carbon Nanotubes. *Nat. Nanotechnol.* **2009**, *4*, 64–70.
6. Green, A. A.; Hersam, M. C. Colored Semitransparent Conductive Coatings Consisting of Monodisperse Metallic Single-Walled Carbon Nanotubes. *Nano Lett.* **2008**, *8*, 1417–1422.
7. Kiowski, O.; Arnold, K.; Lebedkin, S.; Hennrich, F.; Kappes, M. M. Direct Observation of Deep Excitonic States in the Photoluminescence Spectra of Single-Walled Carbon Nanotubes. *Phys. Rev. Lett.* **2007**, *99*, 237402.
8. Qian, H. H.; Georgi, C.; Anderson, N.; Green, A. A.; Hersam, M. C.; Novotny, L.; Hartschuh, A. Exciton Energy Transfer in Pairs of Single-Walled Carbon Nanotubes. *Nano Lett.* **2008**, *8*, 1363–1367.
9. Harutyunyan, H.; Gokus, T.; Green, A. A.; Hersam, M. C.; Allegrini, M.; Hartschuh, A. Defect-Induced Photoluminescence from Dark Excitonic States in Individual Single-Walled Carbon Nanotubes. *Nano Lett.* **2009**, *9*, 2010–2014.
10. Ma, Y. Z.; Graham, M. W.; Fleming, G. R.; Green, A. A.; Hersam, M. C. Ultrafast Exciton Dephasing in Semiconducting Single-Walled Carbon Nanotubes. *Phys. Rev. Lett.* **2008**, *101*, 217402.
11. Liu, J.; Hersam, M. C. Recent Developments in Carbon Nanotube Sorting and Selective Growth. *MRS Bull.* **2010**, *35*, 315–321.
12. Kitiyanan, B.; Alvarez, W. E.; Harwell, J. H.; Resasco, D. E. Controlled Production of Single-Wall Carbon Nanotubes by Catalytic Decomposition of CO on Bimetallic Co−Mo Catalysts. *Chem. Phys. Lett.* **2000**, *317*, 497–503.
13. Harutyunyan, A. R.; Chen, G. G.; Paronyan, T. M.; Pigos, E. M.; Kuznetsov, O. A.; Hewaparakrama, K.; Kim, S. M.; Zakharov, D.; Stach, E. A.; Sumanasekera, G. U. Preferential Growth of Single-Walled Carbon Nanotubes with Metallic Conductivity. *Science* **2009**, *326*, 116–120.
14. Hersam, M. C. Progress Towards Monodisperse Single-Walled Carbon Nanotubes. *Nat. Nanotechnol.* **2008**, *3*, 387–394.
15. Tanaka, T.; Jin, H. H.; Miyata, Y.; Kataura, H. High-Yield Separation of Metallic and Semiconducting Single-Wall Carbon Nanotubes by Agarose Gel Electrophoresis. *Appl. Phys. Express* **2008**, *1*, 114001.
16. Tanaka, T.; Jin, H.; Miyata, Y.; Fujii, S.; Suga, H.; Naitoh, Y.; Minari, T.; Miyadera, T.; Tsukagoshi, K.; Kataura, H. Simple and Scalable Gel-Based Separation of Metallic and Semiconducting Carbon Nanotubes. *Nano Lett.* **2009**, *9*, 1497–1500.
17. Moshammer, K.; Hennrich, F.; Kappes, M. M. Selective Suspension in Aqueous Sodium Dodecyl Sulfate According to Electronic Structure Type Allows Simple Separation of Metallic from Semiconducting Single-Walled Carbon Nanotubes. *Nano Res.* **2009**, *2*, 599–606.
18. Ghosh, S.; Bachilo, S. M.; Weisman, R. B. Advanced Sorting of Single-Walled Carbon Nanotubes by Nonlinear Density-Gradient Ultracentrifugation. *Nat. Nanotechnol.* **2010**, *5*, 443–450.
19. Nish, A.; Hwang, J. Y.; Doig, J.; Nicholas, R. J. Highly Selective Dispersion of Singlewalled Carbon Nanotubes Using Aromatic Polymers. *Nat. Nanotechnol.* **2007**, *2*, 640–646.
20. Zheng, M.; Jagota, A.; Strano, M. S.; Santos, A. P.; Barone, P.; Chou, S. G.; Diner, B. A.; Dresselhaus, M. S.; McLean, R. S.; Onoa, G. B.; *et al*. Structure-Based Carbon Nanotube Sorting by Sequence-Dependent DNA Assembly. *Science* **2003**, *302*, 1545–1548.
21. Tu, X. M.; Manohar, S.; Jagota, A.; Zheng, M. DNA Sequence Motifs for Structure-Specific Recognition and Separation of Carbon Nanotubes. *Nature* **2009**, *460*, 250–253.
22. Ju, S. Y.; Doll, J.; Sharma, I.; Papadimitrakopoulos, F. Selection of Carbon Nanotubes with Specific Chiralities Using Helical Assemblies of Flavin Mononucleotide. *Nat. Nanotechnol.* **2008**, *3*, 356–362.
23. Green, A. A.; Hersam, M. C. Ultracentrifugation of Single-Walled Nanotubes. *Mater. Today* **2007**, *10*, 59–60.
24. Arnold, M. S.; Suntivich, J.; Stupp, S. I.; Hersam, M. C. Hydrodynamic Characterization of Surfactant Encapsulated Carbon Nanotubes Using an Analytical Ultracentrifuge. *ACS Nano* **2008**, *2*, 2291–2300.
25. Quintilla, A.; Hennrich, F.; Lebedkin, S.; Kappes, M. M.; Wenzel, W. Influence of Endohedral Water on Diameter Sorting of Single-Walled Carbon Nanotubes by Density Gradient Centrifugation. *Phys. Chem. Chem. Phys.* **2010**, *12*, 902–908.
26. Niyogi, S.; Densmore, C. G.; Doom, S. K. Electrolyte Tuning of Surfactant Interfacial Behavior for Enhanced Density-Based Separations of Single-Walled Carbon Nanotubes. *J. Am. Chem. Soc.* **2009**, *131*, 1144–1153.
27. Carvalho, E. J. F.; dos Santos, M. C. Role of Surfactants in Carbon Nanotubes Density Gradient Separation. *ACS Nano* **2010**, *4*, 765–770.
28. Moghimi, S. M.; Hunter, A. C. Poloxamers and Poloxamines in Nanoparticle Engineering and Experimental Medicine. *Trends Biotechnol.* **2000**, *18*, 412–420.

29. Alvarez-Lorenzo, C.; Gonzalez-Lopez, J.; Fernandez-Tarrio, M.; Sandez-Macho, I.; Concheiro, A. Tetronic Micellization, Gelation and Drug Solubilization: Influence of pH and Ionic Strength. *Eur. J. Pharm. Biopharm.* **2007**, *66*, 244–252.
30. Cherukuri, P.; Gannon, C. J.; Leeuw, T. K.; Schmidt, H. K.; Smalley, R. E.; Curley, S. A.; Weisman, R. B. Mammalian Pharmacokinetics of Carbon Nanotubes Using Intrinsic Near-Infrared Fluorescence. *Proc. Natl. Acad. Sci. U.S.A.* **2006**, *103*, 18882–18886.
31. Mutlu, G. M.; Budinger, G. R. S.; Green, A. A.; Urich, D.; Soberanes, S.; Chiarella, S. E.; Alheid, G. F.; McCrimmon, D. R.; Szleifer, I.; Hersam, M. C. Biocompatible Nanoscale Dispersion of Single-Walled Carbon Nanotubes Minimizes *in Vivo* Pulmonary Toxicity. *Nano Lett.* **2010**, *10*, 1664–1670.
32. Shvartzman-Cohen, R.; Florent, M.; Goldfarb, D.; Szleifer, I.; Yerushalmi-Rozen, R. Aggregation and Self-Assembly of Amphiphilic Block Copolymers in Aqueous Dispersions of Carbon Nanotubes. *Langmuir* **2008**, *24*, 4625–4632.
33. Florent, M.; Shvartzman-Cohen, R.; Goldfarb, D.; Yerushalmi-Rozen, R. Self-Assembly of Pluronic Block Copolymers in Aqueous Dispersions of Single-Wall Carbon Nanotubes As Observed by Spin Probe EPR. *Langmuir* **2008**, *24*, 3773–3779.
34. Shvartzman-Cohen, R.; Nativ-Roth, E.; Baskaran, E.; Levi-Kalisman, Y.; Szleifer, I.; Yerushalmi-Rozen, R. Selective Dispersion of Single-Walled Carbon Nanotubes in the Presence of Polymers: The Role of Molecular and Colloidal Length Scales. *J. Am. Chem. Soc.* **2004**, *126*, 14850–14857.
35. Nativ-Roth, E.; Shvartzman-Cohen, R.; Bounioux, C.; Florent, M.; Zhang, D. S.; Szleifer, I.; Yerushalmi-Rozen, R. Physical Adsorption of Block Copolymers to SWNT and MWNT: A Nonwrapping Mechanism. *Macromolecules* **2007**, *40*, 3676–3685.
36. Nagarajan, R.; Bradley, R. A.; Nair, B. R. Thermodynamically Stable, Size Selective Solubilization of Carbon Nanotubes in Aqueous Solutions of Amphiphilic Block Copolymers. *J. Chem. Phys.* **2009**, *131*, 104906.
37. Moore, V. C.; Strano, M. S.; Haroz, E. H.; Hauge, R. H.; Smalley, R. E.; Schmidt, J.; Talmon, Y. Individually Suspended Single-Walled Carbon Nanotubes in Various Surfactants. *Nano Lett.* **2003**, *3*, 1379–1382.
38. Dukovic, G.; Balaz, M.; Doak, P.; Berova, N. D.; Zheng, M.; McLean, R. S.; Brus, L. E. Racemic Single-Walled Carbon Nanotubes Exhibit Circular Dichroism When Wrapped with DNA. *J. Am. Chem. Soc.* **2006**, *128*, 9004–9005.
39. Green, A. A.; Duch, M. C.; Hersam, M. C. Isolation of Single-Walled Carbon Nanotube Enantiomers by Density Differentiation. *Nano Res.* **2009**, *2*, 69–77.
40. Arnold, M. S.; Stupp, S. I.; Hersam, M. C. Enrichment of Single-Walled Carbon Nanotubes by Diameter in Density Gradients. *Nano Lett.* **2005**, *5*, 713–718.
41. O'Connell, M. J.; Bachilo, S. M.; Huffman, C. B.; Moore, V. C.; Strano, M. S.; Haroz, E. H.; Rialon, K. L.; Boul, P. J.; Noon, W. H.; Kittrell, C.; *et al*. Band Gap Fluorescence from Individual Single-Walled Carbon Nanotubes. *Science* **2002**, *297*, 593–596.
42. Li-Ping, Y.; Cai-Yuan, P. A Non-covalent Method to Functionalize Multiwalled Carbon Nanotubes Using Six-Armed Star Poly(L-lactic acid) with a Triphenylene Core. *Macromol. Chem. Phys.* **2008**, 783–793.
43. Li, H. G.; Liu, C. C.; Hao, J. C.; Hartnagel, U.; Hirsch, A. Dispersing Carbon Nanotubes by Star-Like Water Soluble C-60 Derivatives. *J. Nanosci. Nanotechnol.* **2009**, *9*, 2763–2767.
44. Kusner, I.; Srebnik, S. Conformational Behavior of Semi-Flexible Polymers Confined to a Cylindrical Surface. *Chem. Phys. Lett.* **2006**, *430*, 84–88.
45. Gurevitch, I.; Srebnik, S. Conformational Behavior of Polymers Adsorbed on Nanotubes. *J. Chem. Phys.* **2008**, *128*, 144901.
46. Gurevitch, I.; Srebnik, S. Monte Carlo Simulation of Polymer Wrapping of Nanotubes. *Chem. Phys. Lett.* **2007**, *444*, 96–100.
47. Liu, Z.; Cai, W.; He, L.; Nakayama, N.; Chen, K.; Sun, X.; Chen, X.; Dai, H. *In Vivo* Biodistribution and Highly Efficient Tumour Targeting of Carbon Nanotubes in Mice. *Nat. Nanotechnol.* **2007**, *2*, 47–52.